J. Fluid Mech. (1984), *vol.* 139, *pp.* 237–260
Printed in Great Britain

A nonlinear convective system with oscillatory behaviour for certain parameter regimes

By PETER LUNDBERG AND LARS RAHM
Department of Oceanography, University of Gothenburg,
Box 4038, S-40040 Gothenburg, Sweden

(Received 29 June 1982 and in revised form 7 October 1983)

The behaviour of a fluid system governed by a quadratic equation of state for the temperature is studied. The model consists of two well-mixed and interconnected vessels subjected to external thermal forcing. If inertial effects are neglected the temperature response of the fluid is governed by two autonomous ordinary differential equations in time. An investigation of these equations revealed that, depending upon the choice of parameters, the system has two possible final states: one stationary, the other a relaxation oscillation. The transitions between these states occur as sub- and supercritically unstable Hopf bifurcations. For certain parameter ranges, a stationary solution can thus coexist with a relaxation oscillation, the initial conditions determining which of these is realized.

1. Introduction

It has become evident that one fruitful approach to a greater understanding of the physics of complex nonlinear fluid-dynamical systems lies in a simplification of the system under consideration to the point of containing the nonlinear mechanisms only in their most basic forms. Moreover it is often possible, using a Galerkin representation, to simplify the governing equations to a small set of ordinary differential equations in time while hoping that the gross qualitative properties of the complete solution will not be lost. This approach has been successfully used by, for example, Lorenz (1960), Vickroy & Dutton (1979) and Pedlosky & Frenzen (1980) for dealing with models of atmospheric flow. The same technique has been utilized in deriving the Lorenz (1963) model from the partial differential equations governing two-dimensional Rayleigh–Bénard convection. Note, however, that for certain classes of fluid-dynamical problems the spatial dependence of the solutions can be eliminated by formulating the problem in terms of well-mixed connected reservoirs, as demonstrated by Stommel (1961) and Stommel & Rooth (1968), and further extended by Welander in a series of papers (cf. Welander 1981). The success of the general approach in the examples quoted above is indisputable and the theory for dynamical systems as used has proved to be a very efficient tool for handling the nonlinearities.

The aim of this paper is to present some results pertaining to the behaviour of a simple thermodynamical system based on convection in two well-mixed and connected reservoirs. The choice of geometry was dictated by a wish to make the system experimentally realizable, and resulted in two vessels connected with pipes in their upper and lower parts and capable of exchanging heat but not matter with the surroundings. The environment with which the system interacts is not in equilibrium in that it is composed of two reservoirs of different temperatures, each coupled to

one of the vessels by Newtonian heat conduction. Keeping the maximum density properties of water in mind, the working fluid in addition to being viscous is assumed to obey a quadratic law of state with regard to the temperature. The fluid is kept in a well-mixed and thus thermally homogeneous state within each vessel by externally imposed stirring. Since we moreover neglect thermal diffusion through the pipes connecting the vessels, we have a closed system from which all spatial dependence has been eliminated.

The governing equations which result from this model form a nonlinear autonomous system of two ordinary differential equations in time for the temperatures within the vessels. This system, which can be regarded as being forced by the non-equilibrium environment, is capable of utilizing the resulting energy flux to organize various modes of circulation. Each of these can under non-equilibrium conditions only be maintained by an adequate flow of energy through the system. A mathematical analysis of the problem has been undertaken, and §2 will deal with analytical results concerning the qualitative behaviour of the degenerate case when the system is thermally insulated from the environment. In §3 the complete problem is formulated and some results on the existence and stability of the critical points are derived. Moreover, a general result concerning the stability of solutions far from equilibrium is established and the qualitative behaviour of these solutions as they approach the region to which they are thermodynamically constrained as time grows beyond limits is discussed. In §4 the qualitative behaviour of the complete system within this region is examined, and it will be shown that the system can exhibit either transient behaviour in adjusting to a stationary state or self-sustained oscillations. The bifurcations between these two states are also examined in some detail. In §5 a general discussion of the results attained is undertaken and some of the prospects for future work in the field are outlined.

2. Investigations of a simplified system

The main subject of this paper is the forced dissipative system briefly described above, but in order to facilitate the forthcoming investigation we first consider the degenerate case of the system kept thermally insulated from its environment.

The physical model, illustrated in figure 1, is based upon two vessels of equal height H and of volumes V_1 and V_2. These contain a non-Boussinesq fluid of temperatures T_1^* and T_2^* respectively, the fluid within each vessel assumed to be well mixed as illustrated in the figure by the propellers. The energy input due to this mixing, which raises the potential energy level of the system, is, however, neglected in the analysis. The working fluid is assumed to obey the following equation of state for the density ρ:

$$\rho = \rho_0\{1-\alpha'(T^*-T_0^*)^2\}, \tag{2.1}$$

where α' is the coefficient of thermal expansion and ρ_0 is the reference density associated with the temperature T_0^*. (In what follows T_0^* for analytical simplicity is taken to be zero.) The entire system is subject to a gravitational acceleration g, and the vessels are coupled to one another at their upper and lower boundaries by two circular tubes of radius r and length $\frac{1}{2}l$. A density difference proportional to $T_1^{*2}-T_2^{*2}$ will drive a flow through the lower tube, whereas the upper tube acts like a passive conduit with the sole purpose of ensuring continuity inasmuch as the system is closed. Since the adjustment time of this flow under normal circumstances ($\pi r^2 l \ll \min(V_1, V_2)$)

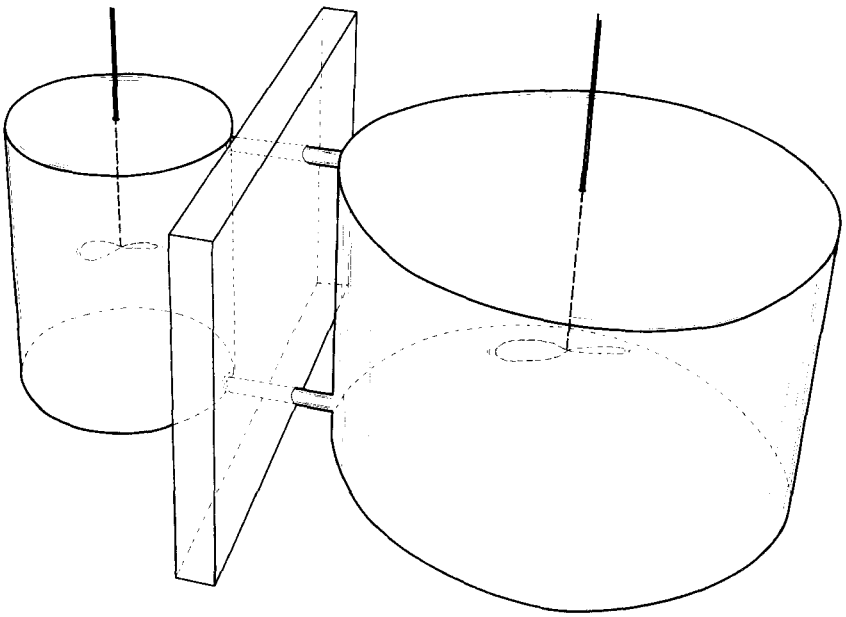

FIGURE 1. Schematic illustration of the physical model, which consists of two interconnected vessels of equal height, each containing a well-mixed fluid. The separating wall indicates the possibility of applying differential thermal forcing.

is much shorter than that of the temperatures T_1^* and T_2^*, we assume that the flow q obeys the law of Hagen–Poiseuille (Landau & Lifschitz 1963):

$$q = \frac{\pi r^4 g\alpha' H}{8\nu l}(T_2^{*2} - T_1^{*2}), \tag{2.2}$$

where ν is the kinematic viscosity of the fluid.

The system is taken to be thermally insulated from its environment, and, since heat can only be advected between the vessels, continuity yields the following equations governing the thermal response of the fluid within each vessel:

$$V_1 \frac{\mathrm{d}T_1^*}{\mathrm{d}t^*} = \frac{\pi r^4 g\alpha' H}{8\nu l}|T_2^{*2} - T_1^{*2}|\,(T_2^* - T_1^*), \tag{2.3a}$$

$$V_2 \frac{\mathrm{d}T_2^*}{\mathrm{d}t^*} = -\frac{\pi r^4 g\alpha' H}{8\nu l}|T_2^{*2} - T_1^{*2}|\,(T_2^* - T_1^*). \tag{2.3b}$$

Here we note that the direction of the flow q is insignificant for the thermal response of the system. We now non-dimensionalize this set of equations according to

$$t^* = t\tau, \quad T_{1,2}^* = T_{1,2}\Delta T, \tag{2.4}$$

where τ is the relaxation time of the system and ΔT is the initial temperature difference $T_2^{*\,\mathrm{init}} - T_1^{*\,\mathrm{init}}$. (Note that this latter scaling breaks down for the case of isothermal initial conditions, but this is of no consequence since these initial states

lead to trivial solutions identical with the initial values.) The governing equations in non-dimensionalized form become

$$\frac{\mathrm{d}T_1}{\mathrm{d}t} = \frac{Ra^*}{\delta}|T_2^2 - T_1^2|\,(T_2 - T_1), \tag{2.5a}$$

$$\frac{\mathrm{d}T_2}{\mathrm{d}t} = -Ra^*|T_2^2 - T_1^2|\,(T_2 - T_1), \tag{2.5b}$$

where $Ra^* = \pi\tau\alpha' r^4 gH(\Delta T)^2/8\nu l V_2$ is a dimensionless quantity, reminiscent of a Rayleigh number, reflecting the magnitude of the initially imposed forcing as compared with the damping inherent in the system. The ratio of the volumes of the vessels is $\delta = V_1/V_2$, $0 < \delta < \infty$.

This two-dimensional autonomous system of ordinary differential equations in time constitutes together with the conditions $T_1(0) = T_1^{\mathrm{init}}$ and $T_2(0) = T_2^{\mathrm{init}}$ an initial-value problem which has two critical points, (i.e. stationary solutions $(T_1^{\mathrm{c}}, T_2^{\mathrm{c}})$ characterized by $\mathrm{d}(T_1^{\mathrm{c}}, T_2^{\mathrm{c}})/\mathrm{d}t = 0$), both of which are located on the diagonals in (T_1, T_2)-space. Conservation of heat yields for $\delta \neq 1$

$$T_1^{\mathrm{c}} = T_2^{\mathrm{c}} = \frac{\delta}{1+\delta}T_1^{\mathrm{init}} + \frac{1}{1+\delta}T_2^{\mathrm{init}}, \tag{2.6a}$$

$$T_1^{\mathrm{c}} = -T_2^{\mathrm{c}} = \frac{\delta}{1-\delta}T_1^{\mathrm{init}} + \frac{1}{1-\delta}T_2^{\mathrm{init}}; \tag{2.6b}$$

and for $\delta = 1$

$$T_1^{\mathrm{c}} = T_2^{\mathrm{c}} = \tfrac{1}{2}(T_1^{\mathrm{init}} + T_2^{\mathrm{init}}), \tag{2.7a}$$

$$T_1^{\mathrm{c}} = -T_2^{\mathrm{c}} = T_1^{\mathrm{init}} = -T_2^{\mathrm{init}}. \tag{2.7b}$$

Note that, in the case of equal volumes of the vessels ($\delta = 1$), a prerequisite for the existence of a critical point located on the antisymmetrical diagonal is that the initial temperatures be of equal magnitude but opposite in sign.

In order to determine the stability of the critical points, the set of governing equations is perturbed with small α and β around the stationary solution in question:

$$T_1 = T_1^{\mathrm{c}} + \alpha, \quad T_2 = T_2^{\mathrm{c}} + \beta. \tag{2.8}$$

For an isothermal critical point ($T_1^{\mathrm{c}} = T_2^{\mathrm{c}}$) the equations governing the perturbations for all δ turn out to be

$$\frac{\mathrm{d}\alpha}{\mathrm{d}t} = \frac{Ra^*}{\delta}|2T_2^{\mathrm{c}}(\beta-\alpha) + (\beta^2-\alpha^2)|\,(\beta-\alpha), \tag{2.9a}$$

$$\frac{\mathrm{d}\beta}{\mathrm{d}t} = -Ra^*|2T_2^{\mathrm{c}}(\beta-\alpha) + (\beta^2-\alpha^2)|\,(\beta-\alpha). \tag{2.9b}$$

By neglecting cubic terms in α and β, these equations can be reformulated as:

$$\frac{\mathrm{d}}{\mathrm{d}t}(\beta-\alpha) = -\mathrm{sgn}\,(T_2^{\mathrm{c}}(\beta-\alpha))\,2Ra^*T_2^{\mathrm{c}}\left(1+\frac{1}{\delta}\right)(\beta-\alpha)^2, \tag{2.10}$$

which in turn is recognized as a degenerate version of the Riccati equation (cf. Ince 1926) with the following general solution:

$$\beta(t)-\alpha(t) = \left\{\mathrm{sgn}\,(T_2^{\mathrm{c}}(\beta(0)-\alpha(0))\,2Ra^*T_2^{\mathrm{c}}\left(1+\frac{1}{\delta}\right)t + C_1\right\}^{-1}, \tag{2.11}$$

where C_1 is an arbitrary constant. Note that the initial values of α and β determine

the sign of the difference between the perturbations at all later times, since in order to change sign the solution must pass through a critical point on the diagonal $T_1 = T_2$. The explicit solution yields that the limiting value of $\beta - \alpha$ is equal to zero, i.e. for increasing time the system approaches a new stationary solution situated on the isothermal diagonal in (T_1, T_2)-space. (Only for an exceptional choice of initial perturbations $\alpha(0)\, V_1 + \beta(0)\, V_2 = 0$ can we expect the system to regain its original critical point (T_1^c, T_2^c).)

A perturbation analysis for the critical points constituting the antisymmetrical diagonal $T_1 = -T_2$ yields the following system of linearized equations:

$$\frac{\mathrm{d}\alpha}{\mathrm{d}t} = \operatorname{sgn}(T_2^c(\alpha+\beta))\frac{Ra^*}{\delta} 4T_2^{c2}(\alpha+\beta), \tag{2.12a}$$

$$\frac{\mathrm{d}\beta}{\mathrm{d}t} = -\operatorname{sgn}(T_2^c(\alpha+\beta))\, Ra^* 4T_2^{c2}(\alpha+\beta). \tag{2.12b}$$

The solution for the sum of the perturbations is found to be

$$\alpha(t)+\beta(t) = C_2 \exp\left\{\operatorname{sgn}(T_2^c(\alpha(0)+\beta(0)))\, 4T_2^{c2}\, Ra^*\left(\frac{1}{\delta}-1\right)t\right\}, \tag{2.13}$$

where C_2 is an arbitrary constant and $\operatorname{sgn}(T_2^c(\alpha+\beta))$ as in the previous case is determined by its initial value. Thus for $\delta \neq 1$ the stationary solution $T_1^c = -T_2^c$ is stable for small perturbations (α, β) such that $(1/\delta - 1)\operatorname{sgn}(T_2^c(\alpha(0)+\beta(0)))$ is negative, whereas a positive value of this quantity yields an unstable critical point. From a physical viewpoint this is not surprising, since in general a temperature perturbation of the system in the steady state $T_1^c = -T_2^c$ can be expected to give rise to a flow which tends to reinforce the temperature imbalance, thus bringing about an instability. However, when the vessels are not of equal volume ($\delta \neq 1$), the thermal response to the flow induced by the initial temperature perturbation differs between the two containers. Thus when $\delta < 1$ for small initial perturbations $\alpha(0)$, $\beta(0)$ such that $\alpha(0)+\beta(0) < 0$ if $T_2^c > 0$ or $\alpha(0)+\beta(0) > 0$ if $T_2^c < 0$, there arises the possibility that the resulting flow counteracts the perturbations, thereby leading to a stable steady state. Analogous conditions prevail when $\delta > 1$. This mechanism, arising from the lack of inertia in the system, is, however, dependent upon the asymmetry of the volumes δ and consequently is not applicable for $\delta = 1$. In the case of equal volumes of the vessels, the full nonlinear perturbation problem ($\alpha(0)+\beta(0) \neq 0$) for the critical point on the antisymmetrical diagonal proves to have an exact solution

$$\begin{aligned}\alpha(t) = T_2^c + \tfrac{1}{2}(\alpha(0)+\beta(0)) - \{2(2T_2^c - \alpha(0)+\beta(0))^{-1} \\ + \operatorname{sgn}((\alpha(0)+\beta(0))(2T_2^c - \alpha(0)+\beta(0)))\, 4(\alpha(0)+\beta(0))\, Ra^* t\}^{-1},\end{aligned} \tag{2.14a}$$

$$\beta(t) = \alpha(0)+\beta(0)-\alpha(t). \tag{2.14b}$$

Since this result is valid irrespective of the initial magnitudes of the perturbations, it in fact represents a global solution to (2.5*a*, *b*) for $T_1^{init} \neq -T_2^{init}$. In the limit $t \to \infty$, (2.14*a*, *b*) yield a stable solution on the symmetrical diagonal consistent with heat conservation. Thus for $\delta = 1$ a critical point $T_1^c = -T_2^c$ is unstable for all perturbations $\alpha(0)+\beta(0) \neq 0$, a result compatible with (2.7*b*).

To summarize it might be stated that this analysis of a thermally insulated version of the general problem has shown the importance of the two diagonals $T_1 = \pm T_2$ and has furthermore demonstrated the difference in behaviour of the system in the vicinity of each of them. There is perhaps reason to expect that some of these

characteristics will be carried over to the complete forced and dissipative system, but since we are studying nonlinear processes the general case may in addition exhibit some unexpected properties.

3. The forced dissipative system; some general viewpoints

The complete forced and dissipative system is obtained by introducing a Newtonian heat flux through the walls of the vessels caused by the prescribed external temperatures T_1^{ex} and T_2^{ex}. The governing equations take the following form:

$$V_1 \frac{dT_1^*}{dt^*} = \frac{\pi r^4 g\alpha' H}{8\nu l} |T_2^{*2} - T_1^{*2}| (T_2^* - T_1^*) + \kappa_1 (T_1^{ex} - T_1^*), \tag{3.1a}$$

$$V_2 \frac{dT_2^*}{dt^*} = -\frac{\pi r^4 g\alpha' H}{8\nu l} |T_2^{*2} - T_1^{*2}| (T_2^* - T_1^*) + \kappa_2 (T_2^{ex} - T_2^*). \tag{3.1b}$$

Here $\kappa_i, i = 1, 2$ is a constant of proportionality defined by the following surface integral over the vessel boundary A_i:

$$\kappa_i = \iint_{A_i} \frac{\hat{K}_i}{\rho_0 C d_i} dA \quad (i = 1, 2), \tag{3.2}$$

where $\hat{K}_i$ is the thermal conductivity of the container wall of thickness d_i, and C is the specific-heat coefficient of the fluid. In order to make the problem analytically tractable we shall in the present paper limit ourselves to the case of $\kappa_1 = \kappa_2 = \kappa$, which in practice is easily realizable since we can prescribe the shapes and thermal characteristics of the vessels. By now redefining $\Delta T = T_2^{ex} - T_1^{ex}$, the previously introduced scaling of the variables results in the following set of non-dimensionalized governing equations:

$$\frac{dT_1}{dt} = \frac{Ra}{\delta} |T_2^2 - T_1^2| (T_2 - T_1) + \frac{1}{\delta Pe} \left(\frac{\theta}{1-\theta} - T_1 \right), \tag{3.3a}$$

$$\frac{dT_2}{dt} = -Ra |T_2^2 - T_1^2| (T_2 - T_1) + \frac{1}{Pe} \left(\frac{1}{1-\theta} - T_2 \right). \tag{3.3b}$$

Here $Ra = \pi\tau\alpha' g H r^4 (\Delta T)^2 / 8\nu l V_2$ is the Rayleigh number, $Pe = V_2/\tau\kappa$ the Péclet number, $\delta = V_1/V_2$ the volume ratio and $\theta = T_1^{ex}/T_2^{ex}$ the ratio of the prescribed external temperatures. Note that $\theta = +1$ gives rise to a singularity in the governing equations due to a breakdown of the scaling. This case, however, lacks physical interest, corresponding as it does to a homothermal steady state, and consequently will be neglected. Given initial conditions, the four parameters Ra, Pe, θ and δ are sufficient to characterize the evolution in time of the entire system. The slightly heterodox definitions of the Rayleigh and Péclet numbers are due to the absence of internal diffusion in the system, whereby the diffusion parameter occurring in these nondimensional numbers must be the one controlling the heat flux through the vessel boundaries.

3.1. *The critical points*

In determining the critical points we first examine the conditions when the expression inside the modulus sign of (3.3a, b) is positive, $T_2^{c2} - T_1^{c2} > 0$. In this case, after elimination of $T_1^c = -T_2^c + (1+\theta)/(1-\theta)$, the equation for T_2^c becomes

$$T_2^{c2} \left(4Ra\, Pe \frac{1+\theta}{1-\theta} \right) + T_2^c \left(1 - 4Ra\, Pe \left(\frac{1+\theta}{1-\theta} \right)^2 \right) + Ra\, Pe \left(\frac{1+\theta}{1-\theta} \right)^3 - \frac{1}{1-\theta} = 0, \tag{3.4}$$

which for $\theta^2 \neq 1$ has the following roots:

$$T_2^c = \frac{1}{2}\frac{1+\theta}{1-\theta} - \frac{1}{8Ra\,Pe}\frac{1-\theta}{1+\theta} \pm \left(\left(\frac{1}{8Ra\,Pe}\frac{1-\theta}{1+\theta}\right)^2 + \frac{1}{4Ra\,Pe(1+\theta)} - \frac{1}{8Ra\,Pe}\right)^{\frac{1}{2}}. \quad (3.5)$$

Since $T_2^{c2} - T_1^{c2}$ *a priori* is taken to be positive, it can be shown that only the positive root is retained. Furthermore it can be demonstrated that the condition $T_2^{c2} - T_1^{c2} > 0$ can be rephrased as $\theta^2 < 1$, i.e. $T_1^{ex2} < T_2^{ex2}$. Thus we obtain the following result for the critical point of our autonomous system of ordinary differential equations when $\theta^2 < 1$:

$$T_1^c = \frac{1}{2}\frac{1+\theta}{1-\theta} + \frac{1}{8Ra\,Pe}\frac{1-\theta}{1+\theta}\left(1 - \left(1 + 8Ra\,Pe\frac{1+\theta}{1-\theta}\right)^{\frac{1}{2}}\right), \quad (3.6a)$$

$$T_2^c = \frac{1}{2}\frac{1+\theta}{1-\theta} - \frac{1}{8Ra\,Pe}\frac{1-\theta}{1+\theta}\left(1 - \left(1 + 8Ra\,Pe\frac{1+\theta}{1-\theta}\right)^{\frac{1}{2}}\right). \quad (3.6b)$$

When $T_2^{c2} - T_1^{c2} < 0$, the equation for T_2^c turns out to be

$$T_2^{c2}\left(4Ra\,Pe\frac{1+\theta}{1-\theta}\right) + T_2^c\left(-1 - 4Ra\,Pe\left(\frac{1+\theta}{1-\theta}\right)^2\right) + Ra\,Pe\left(\frac{1+\theta}{1-\theta}\right)^3 + \frac{1}{1-\theta} = 0. \quad (3.7)$$

In the same manner as above it may now be shown that the condition $T_2^{c2} - T_1^{c2} < 0$ is equivalent to $\theta^2 > 1$, i.e. $T_1^{ex2} > T_2^{ex2}$. Finally we arrive at the following result for the critical point of the system when $\theta^2 > 1$:

$$T_1^c = \frac{1}{2}\frac{1+\theta}{1-\theta} - \frac{1}{8Ra\,Pe}\frac{1-\theta}{1+\theta}\left(1 - \left(1 - 8Ra\,Pe\frac{1+\theta}{1-\theta}\right)^{\frac{1}{2}}\right), \quad (3.8a)$$

$$T_2^c = \frac{1}{2}\frac{1+\theta}{1-\theta} + \frac{1}{8Ra\,Pe}\frac{1-\theta}{1+\theta}\left(1 - \left(1 - 8Ra\,Pe\frac{1+\theta}{1-\theta}\right)^{\frac{1}{2}}\right). \quad (3.8b)$$

The limiting case $T_2^{c2} - T_1^{c2} = 0$, which in practice is equivalent to $\theta = -1$ since we have decided to neglect the trivial case of isothermal forcing $\theta = +1$, has the following critical point:

$$T_1^c = -T_2^c = -\tfrac{1}{2}. \quad (3.9)$$

The critical point (T_1^c, T_2^c) does not depend upon the ratio of the volumes, since these only influence the rates of change of the temperature, which by definition are equal to zero for a stationary solution.

The two general cases discussed above are defined by the ratio θ of the imposed external temperatures T_1^{ex} and T_2^{ex}. A way of recognizing their fundamental unity is to make the *gedanken* experiment of interchanging the two vessels and their thermal forcing; in effect to make the transformation

$$\hat{\theta} = \frac{1}{\theta}, \quad \hat{\delta} = \frac{1}{\delta},$$

which in turn leads to $\hat{Pe} = Pe\,\delta$ and $\hat{Ra} = Ra/\delta$. If now $\theta^2 < 1$, then $\hat{\theta}^2 > 1$, and it is found from the explicit expressions above that $\hat{T}_1^c = -T_2^c$ and $\hat{T}_2^c = -T_1^c$. Since the transformation also affects the temperature scaling, $\Delta\hat{T} = -\Delta T$, this result is in accordance with what might have been expected from a physical standpoint. Keeping this in mind, it is recognized that if δ is allowed to range over the positive part of the real axis no information is lost when we in what follows limit ourselves to studying the case of $T_2^{c2} - T_1^{c2} > 0$, i.e. $\theta^2 < 1$.

3.2. *Global properties of the solution*

In order to determine whether all solutions to the problem are bounded, define a positive definite Liapunov function (cf. Lasalle & Lefschetz 1961) V such that

$$V = \delta T_1^4 + T_2^4. \tag{3.10}$$

The derivative $\mathrm{d}V/\mathrm{d}t$ with respect to our autonomous system of governing differential equations (3.3 a, b) becomes

$$\frac{\mathrm{d}V}{\mathrm{d}t} = 4Ra\{-|T_2^2 - T_1^2|\,(T_2^4 + T_1^4) + |T_2^2 - T_1^2|\,(T_2 T_1^3 + T_1 T_2^3)\} + \frac{4}{Pe}\left\{-(T_1^4 + T_2^4) + \left(T_1^3 \frac{\theta}{1-\theta} + T_2^3 \frac{1}{1-\theta}\right)\right\}. \tag{3.11}$$

Using Cauchy's inequality it is found that the first term on the right-hand side of (3.11) fulfils

$$-4Ra|T_2^2 - T_1^2|\,\{T_1^4 + T_2^4 - T_1 T_2 (T_1^2 + T_2^2)\} \leqslant 0.$$

The second term can be written as

$$-\frac{4}{Pe}\left\{T_1^2\left(T_1^2 - \frac{\theta}{1-\theta} T_1\right) + T_2^2\left(T_2^2 - \frac{1}{1-\theta} T_2\right)\right\},$$

which is negative-definite outside the ellipse

$$K = \delta T_1^4 + T_2^4, \tag{3.12}$$

where K is sufficiently large. Thus $\mathrm{d}V/\mathrm{d}t < 0$ for $V > K$, i.e. trajectories that represent solutions to the forced, dissipative system must ultimately become trapped in the region where

$$\delta T_1^4 + T_2^4 < K. \tag{3.13}$$

Consequently all solutions to the set of governing equations are bounded. (From a physical viewpoint this should come as no surprise, since the external temperature forcing and dissipation constrain the solutions to a well-defined region irrespective of the initial state of the system.) An important consequence is that according to the theorem of Bendixson (Lefschetz 1962) we can expect the solution to the general problem to be periodic in character if the critical point is unstable.

Since the solutions to the general set of governing equations are globally stable, it is possible to glean some information about the system from studying the manner in which arbitrary trajectories approach the region of the origin to which the thermodynamical forcing ultimately constrains the solutions. This is accomplished by numerical integration in time of the governing equations. The algorithm chosen was a fourth-order Kutta–Merson scheme, which provides a measure of the numerical error in each iteration, thus making it possible to keep the relative error within predetermined bounds by varying the time step.

The results from a series of numerical experiments intended to show the behaviour of the system when far from the region of the origin are summarized in the phase plane of figure 2. Here each trajectory represents the evolution in time of the solution associated with a particular set of initial values. Since the initial behaviour of the system proved to be almost insensitive to variations of the parameters, the set of (Ra, Pe, θ, δ) singled out for an investigation yields as representative a phase portrait as any other choice of parameters. From the figure it is evident that, given anisothermal initial conditions, the transient adjustment of the system towards the region of the origin consists of two distinct phases, the first of which is a motion forced

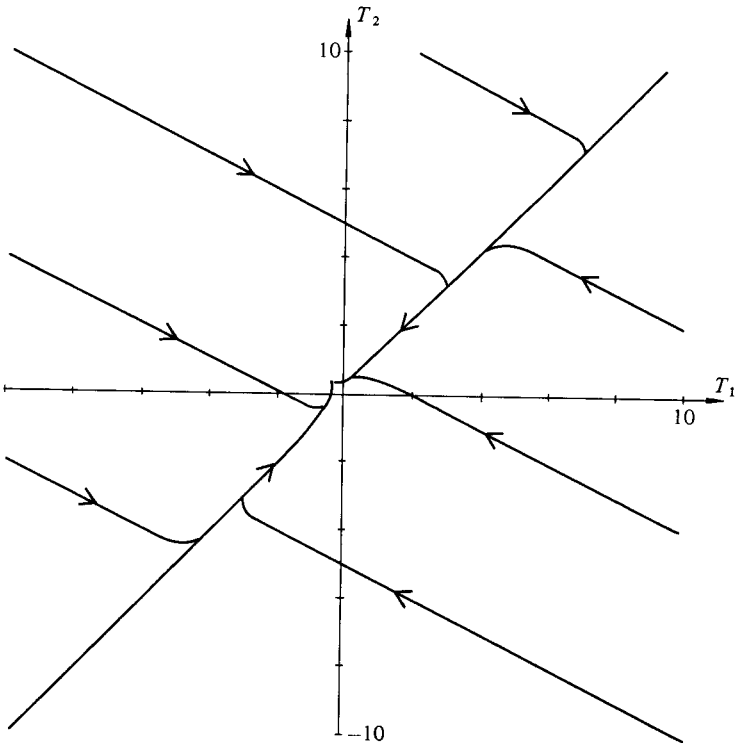

FIGURE 2. In order to illustrate the global behaviour of the system, trajectories of the solutions for varying initial values far from the origin are shown for $Ra = 5$, $Pe = 1$, $\theta = -\frac{13}{14}$ and $\delta = \frac{1}{2}$.

by the initially prescribed temperature difference towards a quasistagnant isothermal state. This adjustment is comparatively rapid, as can be gathered from observations of the dependence of T_1 and T_2 on time in the numerical experiments. Once the solution has reached an isothermal state, a slow motion towards the origin takes place, the pace of which is determined by the external forcing. Only near the origin itself do the trajectories turn away from the isothermal diagonal. To elucidate the behaviour of the solutions hereafter will, however, be the topic of §4.

4. The forced dissipative system; a more detailed investigation

In order to determine the behaviour of the solution in the region close to the origin, a prerequisite is that the stability characteristics of the critical point be fully explored. In the general case of $\theta^2 < 1$, a linear stability analysis yields the following second-degree algebraic equation for the eigenvalues λ determining the stability properties of the critical point (T_1^c, T_2^c):

$$\lambda^2 + \frac{\lambda}{Pe\,\delta}\left\{\frac{\delta-1}{16Ra\,Pe}\left(\frac{1-\theta}{1+\theta}\right)^2\left(1-\left(1+8Ra\,Pe\frac{1+\theta}{1-\theta}\right)^{\frac{1}{2}}\right)^2 - \frac{\delta+1}{2}\left(1-\left(1+8Ra\,Pe\frac{1+\theta}{1-\theta}\right)^{\frac{1}{2}}\right)+\delta+1\right\}+\frac{1}{Pe^2\,\delta}\left(1+8Ra\,Pe\frac{1+\theta}{1-\theta}\right)^{\frac{1}{2}} = 0. \quad (4.1)$$

The zeroth-degree term is positive definite for all non-singular values of the parameters, and consequently the stability of the critical point is determined by the

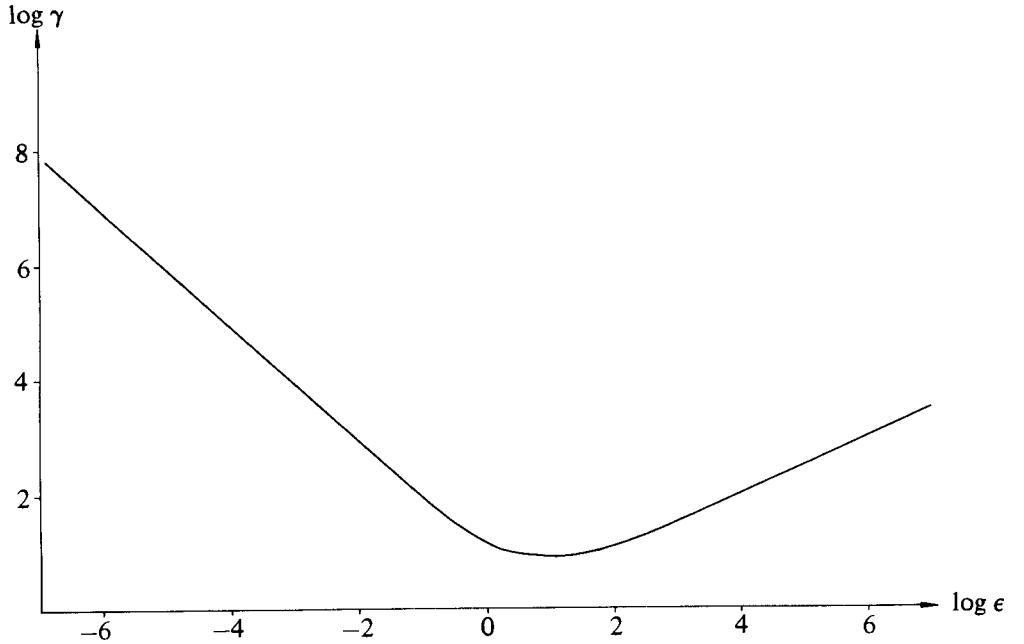

FIGURE 3. Curve separating the 'upper' domain of unstable critical points in (ϵ, γ)-space from the 'lower' stable region.

sign of the first-degree coefficient. Furthermore, owing to the non-zero constant term of the equation, when the eigenvalues are real these are definite in sign even for varying values of the parameters. When the discriminant of the equation is smaller than zero, the eigenvalues are complex and their real parts can change sign. Thus the condition

$$\frac{\delta-1}{\delta+1}\left(\frac{1-\theta}{1+\theta}\right)^2\left(1-\left(1+8Ra\,Pe\frac{1+\theta}{1-\theta}\right)^{\frac{1}{2}}\right)^2 - 8Ra\,Pe\left(1-\left(1+8Ra\,Pe\frac{1+\theta}{1-\theta}\right)^{\frac{1}{2}}\right)+16Ra\,Pe=0, \quad (4.2)$$

separates the domain of unstable critical points in four-dimensional parameter space $(Ra > 0, Pe > 0, \theta^2 < 1, \delta > 0)$ from the stable region. By introducing

$$\epsilon = 8Ra\,Pe\frac{1+\theta}{1-\theta}, \quad \gamma = \frac{1-\delta}{1+\delta}\frac{1-\theta}{1+\theta},$$

the hypersurface above reduces to

$$\gamma = \frac{\epsilon(1+(1+\epsilon)^{\frac{1}{2}})}{(1-(1+\epsilon)^{\frac{1}{2}})^2}. \quad (4.3)$$

This boundary in two-dimensional parameter space ($\epsilon > 0$, $-\infty < \gamma < +\infty$), with a minimum of $\gamma = 8$ for $\epsilon = 8$, is shown in figure 3, where the region above the curve is associated with an unstable critical point. A qualitative change of the solutions to (3.3a, b) occurs for alterations of ϵ and γ such that the boundary is crossed. From the point of view of bifurcation theory it is of great importance to establish the manner

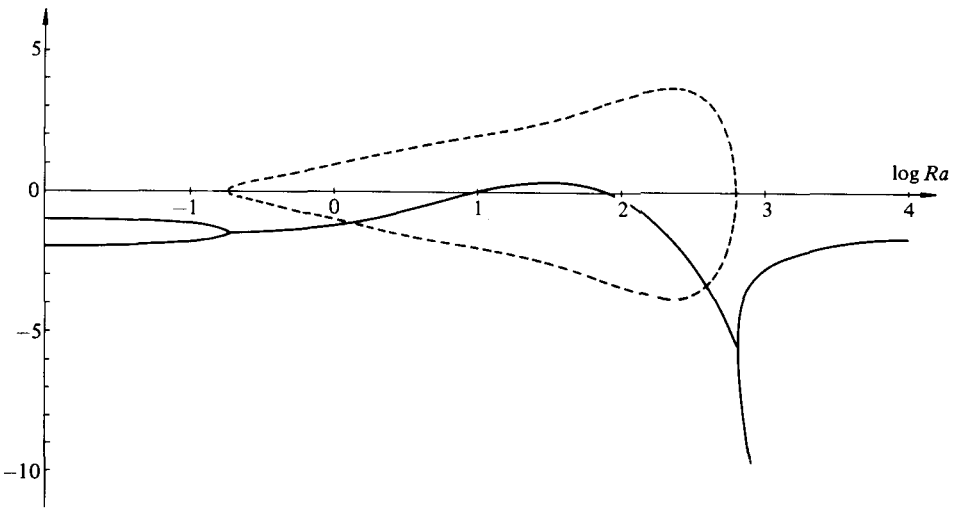

FIGURE 4. Eigenvalues determining the stability of the critical point versus the Rayleigh number for $Pe = 1$, $\theta = -\frac{13}{14}$ and $\delta = \frac{1}{2}$. The full and dashed lines represent the real and imaginary parts respectively.

in which the eigenvalues cross the imaginary axis as the parameter μ selected for investigation is varied. If it can be shown that this occurs transversally,

$$\frac{\partial}{\partial \mu}(Re\,\lambda)_{\mu=\mu_c} \neq 0, \tag{4.4}$$

where μ_c is the critical value of the parameter, the necessary conditions for a Hopf bifurcation, i.e. the emergence of stable or unstable closed orbits of the solution, are fulfilled (cf. Iooss & Joseph 1980). When γ is taken to be the bifurcation parameter the conditions for transversality are satisfied for all ϵ. In order to conform to established practice within the field of thermal convection, interest is, however, focused upon the parameter ϵ, which is proportional to the Rayleigh number. It can be shown that the only parameter values satisfying (4.3), for which the derivative with respect to ϵ of the real part of the eigenvalues vanishes, are $\epsilon = \gamma = 8$. Since this point represents the minimum of the curve in figure 3, it is recognized that the non-transversality is not associated with a proper change of sign of the real part of the eigenvalues as the parameter ϵ is varied, but rather represents the limiting case of the stable critical point becoming neutrally stable before reverting to stability as the bifurcation parameter is further increased. Thus for $\gamma > 8$ both a regular and an inverse Hopf bifurcation occur as the parameter ϵ is increased. The question of the stability of the resulting periodic orbits will, however, be dealt with in a more appropriate context.

A prerequisite for a stagnant steady state $T_1^c = -T_2^c$ is that the thermal forcing be antisymmetrical, i.e. $\theta = -1$. In this case a linear stability analysis for small perturbations α and β around the resulting critical point $T_1^c = -T_2^c = -\frac{1}{2}$ yields the following equation for the eigenvalues λ:

$$\lambda^2 + \lambda\left\{\mathrm{sgn}\,(\alpha+\beta)\,Ra\left(1-\frac{1}{\delta}\right)+\frac{1}{Pe}\left(1+\frac{1}{\delta}\right)\right\}+\frac{1}{Pe^2\delta}=0, \tag{4.5}$$

where the sign of the sum of the perturbations plays a crucial rôle. Note that for

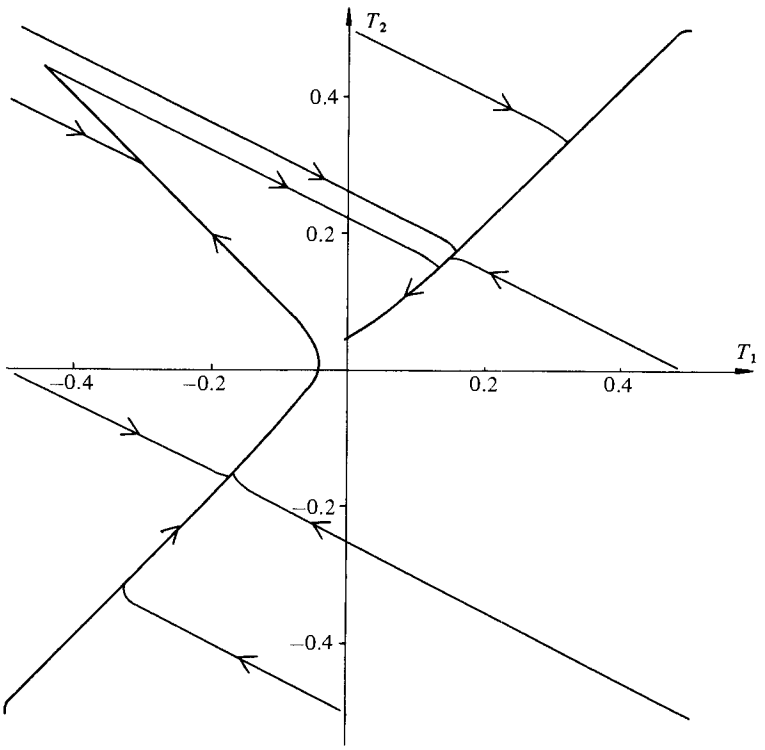

FIGURE 5. Solution trajectories for various initial values close to the origin for strong thermal forcing, $Ra = 5000$, when $Pe = 1$, $\theta = -\frac{13}{14}$ and $\delta = \frac{1}{2}$.

perturbations such that $\alpha+\beta = 0$, an immediate adjustment to a state such that $\alpha+\beta \neq 0$ takes place since $\lambda_1 \neq \lambda_2$ when $\delta \neq 1$, and only for equal volumes of the vessels ($\delta = 1$) does a motion towards the in this case stable critical point take place along the antisymmetrical diagonal. Using the same type of argument as in §2 it can be shown that for the more general case of $\alpha+\beta \neq 0$ there are two regimes where the critical point is unconditionally nodally stable, namely $\alpha+\beta > 0$ & $\delta > 1$ and $\alpha+\beta < 0$ & $\delta < 1$. The boundary case of $\delta = 1$ is always associated with a stable improper node irrespective of the sign of the sum of the perturbations. For the remaining cases the situation is more complex. When $\alpha+\beta > 0$ and $\delta < 1$, the critical point can be either unstable or stable, depending on whether $Ra\,Pe$ is larger or smaller than $(1+\delta)/(1-\delta)$ respectively, the sign of the discriminant of (4.5) determining whether it is nodal or spiral in character. The condition for a spiral point is found to be

$$\frac{(1-\delta^{\frac{1}{2}})^2}{1-\delta} < Ra\,Pe < \frac{(1+\delta^{\frac{1}{2}})^2}{1-\delta}. \tag{4.6}$$

The case $\alpha+\beta < 0$ and $\delta > 1$ is similar, and analogous conditions for the character of the critical point can be derived. A comparison with the results of §2 does not appear unreasonable, since in the degenerate case one of the lines of critical points was indeed $T_1^c = -T_2^c$, the stability properties of which were determined by the sign of the sum of the perturbations. Consequently we note that the existence of thermal forcing can exert a stabilizing influence, since the critical point $T_1^c = -T_2^c = -\frac{1}{2}$ presently under consideration is unconditionally stable for $Ra\,Pe$ smaller than a critical value dependent upon δ. Furthermore, since this stationary solution for a large

enough $Ra\,Pe$ value also is conditionally (with respect to the sign of the sum of the perturbations) unstable, from a practical point of view (stochastic temperature perturbations) it demonstrates some of the characteristics associated with the onset of thermal convection from a stagnant steady state in classical hydromechanics.

Once the stability characteristics of the critical point have been determined, it is possible to discuss the overall behaviour of the solutions, i.e. the manner in which the system adjusts from prescribed initial conditions to either a stationary state or a self-sustained oscillation. Since we wish to examine the dependence of the system upon the Rayleigh number, the parameter ϵ was varied for $\gamma = 9$, a choice which ensured an ϵ-traverse through both stable and unstable regions. This restriction to only one value of γ does not represent any serious limitation, since numerical investigations have indicated that the qualitative behaviour of the system in the phase plane is a generic feature and that the influence of γ primarily manifests itself in the timescales of the problem. However, in the original parameter space several degrees of freedom still remain in that Ra, Pe, θ and δ can assume a multiplicity of values for fixed ϵ and γ. The main part of the forthcoming investigations will be focused upon $Pe = 1$ and $\delta = \frac{1}{2}$, which in turn yields $\theta = -\frac{13}{14}$ for the previously assigned value of γ. This does represent somewhat of a restriction, but, as will be shown, the effects of varying δ for a fixed value of γ limit themselves to quantitative changes of the phase-portraits and do not involve any drastic qualitative alterations of the solutions. In a similar fashion a variation of the Péclet number primarily affects the timescales of the problem. Furthermore, by assigning fixed values to θ and Pe, the traverse in the ϵ-direction becomes solely dependent upon the Rayleigh number. The eigenvalues determining the stability characteristics of the critical point for these parameter values have in figure 4 been graphed as functions of the Rayleigh number. As can be seen there are two distinct regions, analytically determined as $Ra < 10.125$ and $Ra > 81$, where the real parts of the eigenvalues are negative, thereby giving rise to a stable critical point. In the next subsection we shall examine the characteristics of the transient solutions in these parameter ranges.

4.1. *Qualitative behaviour of the solution in the stable-critical-point regime*

The regimes $Ra < 10.125$ and $Ra > 81$ correspond to weak and strong thermal forcing of the system respectively. To gain an understanding of the transient solution as it progresses towards its stationary state for strong thermal forcing, the Rayleigh number is taken to be 5×10^3. In this case the eigenvalues of the characteristic equation are real and negative, and thus the critical point is a stable nodal point, as is also evidenced by the phase portrait shown in figure 5. In §3.2, dealing with the global behaviour of the solutions in the region far from the origin, the prominence of the attracting path in the immediate neighbourhood of the isothermal diagonal was noted. The present phase portrait of the region in the vicinity of the origin demonstrates that for a large Rayleigh number the importance of this attracting path is unchanged, and it will henceforth be referred to as the symmetrical attracting path. Furthermore we note that another attracting path comes into play in this region. It is orientated along the diagonal $T_1 = -T_2$ and represents a quasihydrostatical state of the system, analogous to what was encountered when studying the stationary solutions for the degenerate case of thermally insulated vessels in §2, and in what follows it will be denoted as the antisymmetrical attracting path. However, an important difference between the attracting paths presently under consideration and the critical points situated on $T_1 = \pm T_2$ of §2 is that the external thermal forcing causes a slight shift of the attracting paths from the diagonals proper, a phenomenon

to be examined in greater detail when discussing the physical basis for the behaviour of the solutions. As is evident from the phase plane of figure 5, there are two general routes of approach to the stable critical point. The least devious results in a simple motion along the 'upper' branch of the symmetrical attracting path until the influence of the critical point is felt, whereupon a direct route to the stationary solution is taken. A more complicated route ensues when the trajectories have coalesced with the 'lower' part of the symmetrical attracting path. In this case a motion towards the origin takes place until the allegiance of the trajectories is transferred to the antisymmetrical path, a state which so remains until a drastic jump to the 'upper' part of the symmetrical path occurs. Thereafter the solutions progress in the manner already outlined.

Since the system under consideration is thermodynamically open and moreover lacks thermal diffusion between the vessels, a trajectory coinciding with either diagonal is precluded and consequently the attracting paths are situated a small distance from the diagonals proper. By examining the passage along the symmetrical path, which owing to $\theta < 0$ takes place somewhat above the diagonal $T_1 = T_2$, it is recognized that the motion is stable since an arbitrary but small temperature perturbation of the system is always compensated for by the resulting flow. Furthermore, due to the choice of external thermal forcing ($\theta < 0$) and experimental configuration ($\delta < 1$), any motion along the symmetrical diagonal must be towards the origin. Note that for the antisymmetrical attracting path the interaction between the thermal forcing ($\theta < 0$) and the difference in volumes of the two vessels ($\delta < 1$) leads to the trajectories being situated somewhat below the diagonal itself. The same restoring mechanism as for the symmetrical attracting path causes the motion to be stable for temperature perturbations such that the diagonal $T_1 = -T_2$ is not transgressed. Since the thermodynamics of the system constrain the trajectories to move away from the origin in an almost hydrostatically balanced manner, it is recognized that the prescribed condition of $\theta > -1$ inevitably leads to a crossing of the diagonal (in contrast with the limiting case of $\theta = -1$ discussed earlier in this section, where the point of external thermal forcing coincided with the conditionally semistable critical point situated on the diagonal itself). Once above the diagonal the solutions lose stability since the flow between the vessels, which previously tended to counteract temperature perturbations, now reinforces them in a manner similar to the one outlined in §2. Thereafter an almost adiabatic jump to the symmetrical path ensues. A formal investigation of the stability properties of $(T_1(t), T_2(t))$ in the course of its trajectory can be achieved by considering the behaviour of perturbations superimposed on the solution. Since the perturbations are taken to be small, a linearization of the resulting set of governing equations is valid (cf. Lorenz 1963). The resulting characteristic equation when $T_1^2(t) \neq T_2^2(t)$ for the eigenvalues λ, with in this case time-dependent coefficients, is readily found:

$$\lambda^2 + \left\{\frac{1+\delta}{Pe\,\delta} + \frac{Ra}{\delta}\operatorname{sgn}(T_2^2(t) - T_1^2(t))\,((1+3\delta)\,T_2^2(t) + 2(1-\delta)\,T_2(t)\,T_1(t) - (3+\delta)\,T_1^2(t))\right\}\lambda + \frac{1}{Pe\,\delta}\left\{\frac{1}{Pe} + 4Ra\operatorname{sgn}(T_2^2(t) - T_1^2(t))\,(T_2^2(t) - T_1^2(t))\right\} = 0. \quad (4.7)$$

Since the constant term of this second-degree equation is positive definite, the sign of the first-degree coefficient determines the stability properties of $(T_1(t), T_2(t))$. A numerical test to this effect has been incorporated into the general scheme for integration in time and yielded results in accordance with the mechanistic considerations above. Since the computation were performed with a finite time step, the

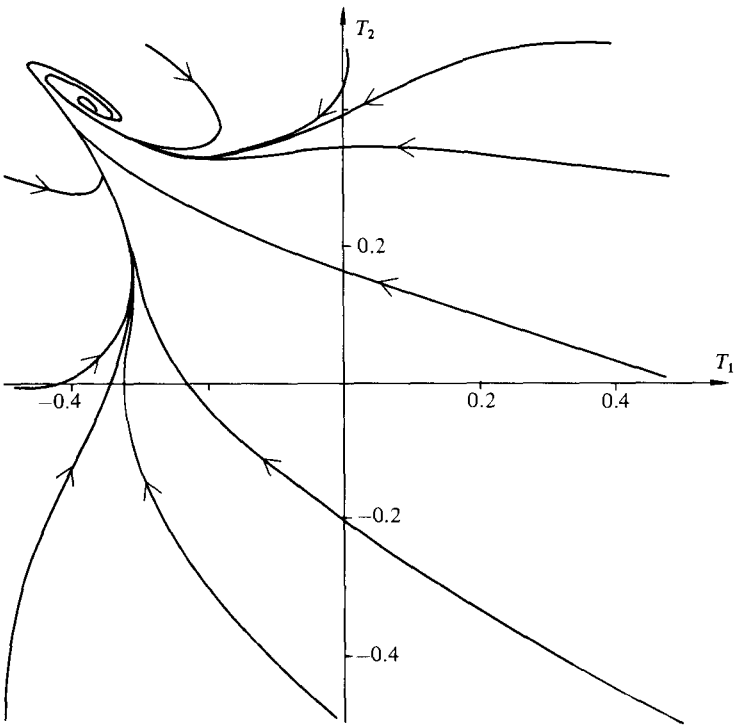

FIGURE 6. Behaviour of solutions for initial values close to the origin for weak thermal forcing, $Ra = 5$, when $Pe = 1$, $\theta = -\frac{13}{14}$ and $\delta = \frac{1}{2}$.

effect of omitting a proper analysis in the instant of $T_1^2(t) = T_2^2(t)$ proved to be totally negligible.

A stable critical point also occurs for weak thermal forcing, $Ra < 10.125$. As in the case of strong thermal forcing, a number of numerical experiments were conducted, but now for $Ra = 5$, and the results are shown in the phase portrait of figure 6. Since the characteristic equation has complex-conjugate roots with negative real parts, the critical point should be spiral in character, and this expectation is borne out by the figure, which furthermore indicates that the two distinct final routes of the trajectories towards the stationary solution are roughly aligned with the diagonal $T_1 = -T_2$. A not-unreasonable interpretation is that the strength of the previously discussed attracting paths has diminished to such an extent that they more or less unnoticeably blend into one another. This has the result that, even though the influence of the attracting paths is evident from the phase portrait, the trajectories take a much less circuitous route towards the stable critical point than was the case for strong thermal forcing. Note that also in the present case there occurs a jump of the solutions from the antisymmetrical path, but it is non-adiabatic as well as rather weak, since $Ra\,Pe$ is small, and forms an integral part of the spiralling motion leading towards the critical point itself. This alteration of the properties of the attracting paths can be understood in terms of the specific balance between advection and thermal forcing which determines the position of the paths as well as their stability properties. Since the effect of advection increases with the distance from the origin in the (T_1, T_2)-plane, owing to its nonlinear dependence upon the temperatures, there is reason to expect the attracting paths to approach the diagonals as T_1 or T_2 increase in magnitude for a fixed value of the Rayleigh number, and indeed this is what is observed in figure

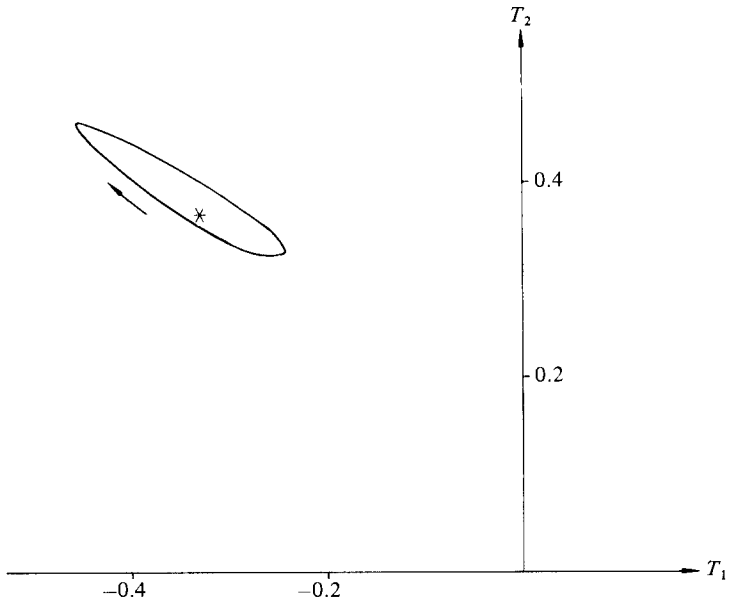

FIGURE 7. Self-sustained periodic solution for $Ra = 8.3$, $Pe = 1$, $\theta = -\frac{13}{14}$ and $\delta = \frac{1}{2}$. The cross indicates the position of the critical point, and the arrows show the evolution in time of the system.

5. However, the advective effects can, as is evident from the governing equations, also be enhanced by an increased value of $Ra\,Pe$ and this is precisely what a comparison between figures 5 and 6 demonstrates. Thus the vague manner in which the attracting paths approach one another and finally coalesce for small values of the Rayleigh number may be attributed to the weak thermal forcing.

4.2. *Qualitative behaviour of the solution in the limit-cycle regime*

As already outlined in §3.2, the global stability of the solutions in conjunction with an unstable critical point for $10.125 < Ra < 81$ leads to the occurrence of limit cycles in the phase plane. Numerical investigations have revealed that for the parameter values under consideration, namely $Pe = 1$, $\theta = -\frac{13}{14}$ and $\delta = \frac{1}{2}$, periodic solutions could be found for $8.25 \lesssim Ra \lesssim 107.85$. In figures 7–9 a selection of the resulting limit cycles is shown. (Since the behaviour of the system for $Ra < 8.25$ has been demonstrated in figure 6, the corresponding approach to the stable critical point for $Ra > 107.85$ is for completeness shown in figure 10.) A salient feature of these phase portraits is the important rôle that the antisymmetrical attracting path plays. For the same reasons that were touched upon in §4.1, a jump from this path also occurs here which carries the phase point to the 'upper' part of the symmetrical attracting path. Owing to the proximity of the origin, the diagonal character of this path is not very pronounced, in accordance with the considerations of §4.1, wherein was furthermore predicted a weakened degree of coincidence between the attracting paths and the diagonals proper for small value of $Ra\,Pe$. This latter effect is clearly borne out by a comparison between figures 7 and 10. A necessary condition for a closed cycle in the phase plane is that a second jump, caused by a loss of stability of the solution on the symmetrical attracting path, takes place back to the antisymmetrical path. This phenomenon is most pronounced in figure 9, but use of the stability criterion derived from (4.7) has shown that the much weaker jumps of figures 7 and 8 are also associated with a loss of stability of the solutions.

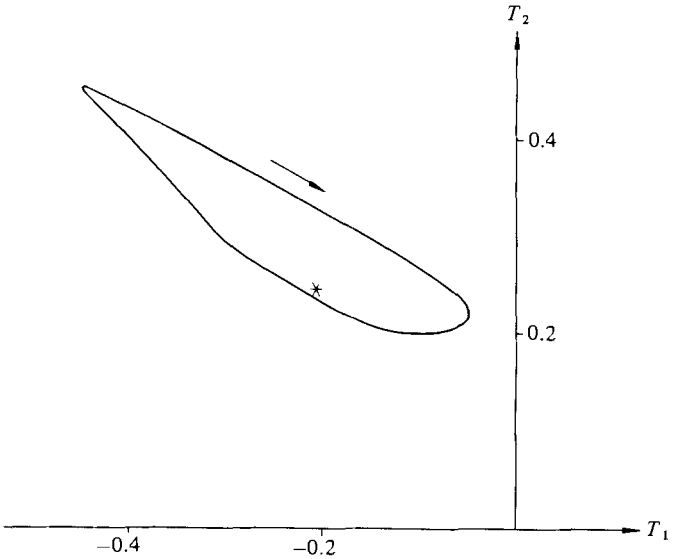

FIGURE 8. As figure 7, but for $Ra = 35.0$.

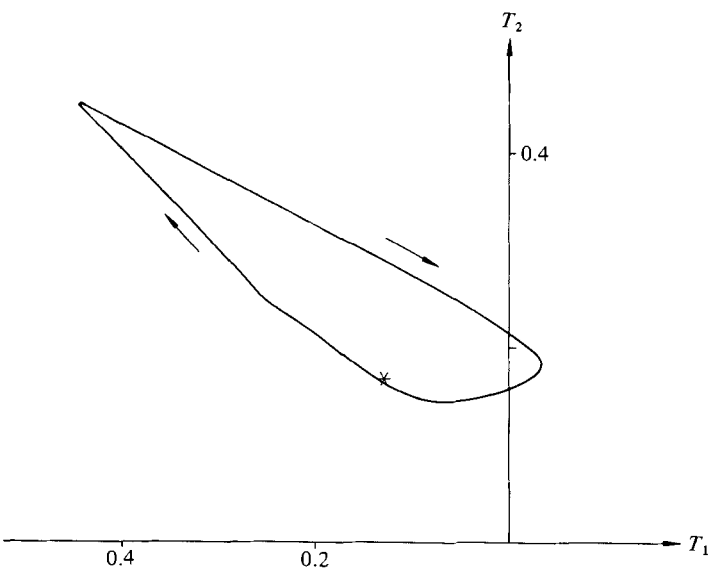

FIGURE 9. As figure 7, but for $Ra = 107.8$.

This oscillatory behaviour is fundamentally nonlinear in that it is inconceivable without a quadratic equation of state, and consequently the system presently under consideration does not represent a nonlinear modification of an essentially linear oscillator. The limit cycle of figures 7–9 is a relaxation oscillation, which in principle is constituted by phases of 'slow' motion (along the two attracting paths) interconnected by 'fast' jumps. Although partly discernible in the phase portraits, these features of the oscillation are particularly evident in figure 11, where $T_1(t)$, $T_2(t)$ and $T_2^2(t) - T_1^2(t)$ have been graphed versus non-dimensional time in the case of a

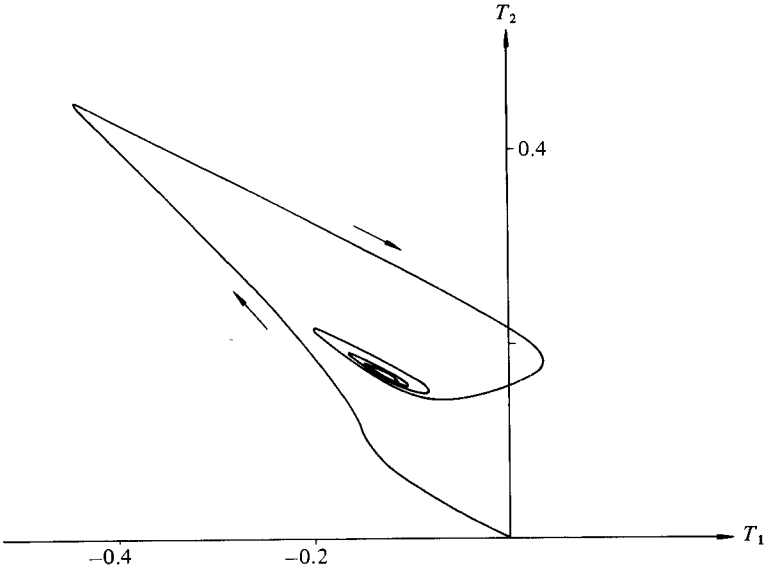

FIGURE 10. Trajectory associated with the initial values $T_1(0) = T_2(0) = 0$ as it approaches the stable critical point for $Ra = 107.9$, $Pe = 1$, $\theta = -\frac{13}{14}$ and $\delta = \frac{1}{2}$.

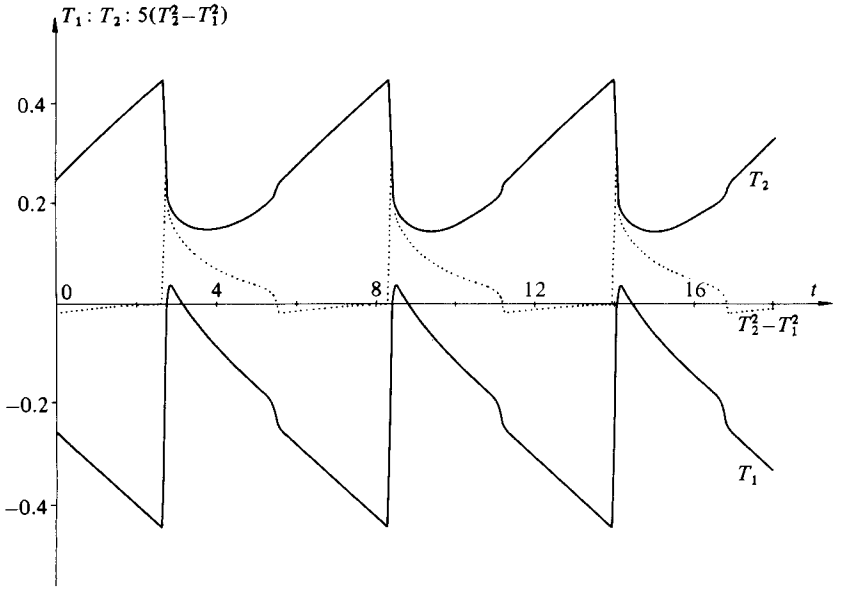

FIGURE 11. $T_1(t)$, $T_2(t)$ and $T_2^2(t)-T_1^2(t)$ versus time for $Ra = 107.5$, $Pe = 1$, $\theta = -\frac{13}{14}$ and $\delta = \frac{1}{2}$.

self-sustained oscillation for $Ra = 107.5$. Here the 'slow' and 'fast' phases of the cycle, corresponding to motion along the attracting paths and the almost-adiabatic jumps respectively, are clearly visible as is the associated behaviour of the volume flux between the vessels.

A peculiarity of the system is that, for $8.25 \lesssim Ra < 10.125$ and $81 < Ra \lesssim 107.85$, a stable critical point can coexist with a limit cycle, the initial values determining which of these states is ultimately realized. This state of affairs is due to the Hopf

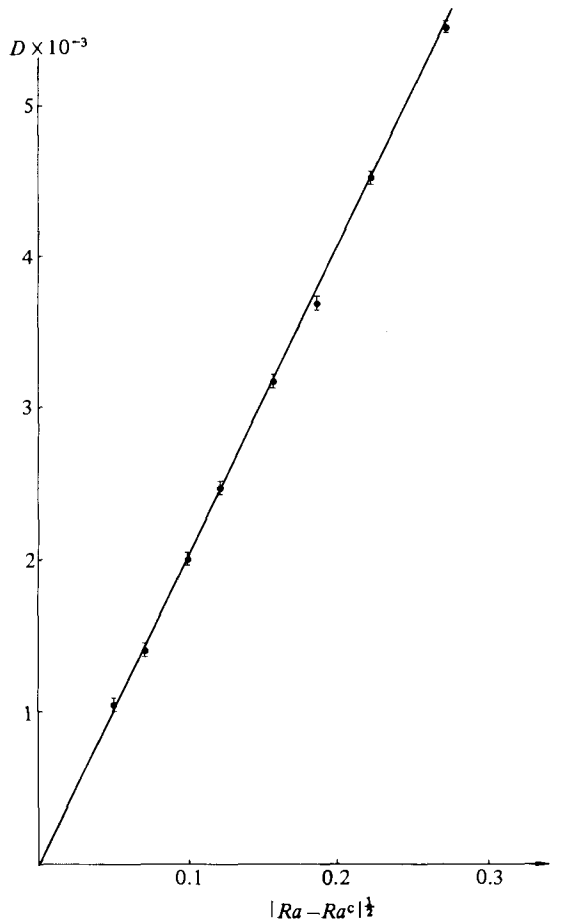

FIGURE 12. Diagram illustrating the linear dependence between the radius D of the repelling orbit associated with the subcritically unstable regular Hopf bifurcation and $|Ra - Ra^c|^{\frac{1}{2}}$, where $Ra^c = 10.125$ is the critical Rayleigh number. The error bars represent the estimated uncertainty in the determination of the radii.

bifurcations at the lower and upper limits of the region of unstable critical points. A formal investigation of the stability properties of the resulting periodic solutions has been undertaken (cf. Marsden & McCracken 1976) and yielded the result that the closed orbits of the regular and inverse Hopf bifurcations were sub- and supercritically unstable respectively, and consequently repelling. This explains the dependence of the final state realized upon the initial values, since the unstable closed orbit serves as a separatrix delimiting an interior region where all solutions finally approach the stable critical point. Even though the orbits resulting from the Hopf bifurcation are unstable, it is possible to investigate their characteristics numerically through the transformation $t \to -t^*$ in the governing equations. An integration along the positive half-path in t^* time can then be performed, ultimately providing an image of the unstable periodic orbit. One of the theoretical predictions (cf. Marsden & McCracken 1976) concerning their behaviour which has been verified is that, in the immediate vicinity of the critical Rayleigh number Ra^c, the radius of the unstable closed orbit is directly proportional to $|Ra - Ra^c|^{\frac{1}{2}}$. This is illustrated in figure 12, which demonstrates the growth of the unstable orbit for the subcritical Hopf bifurcation.

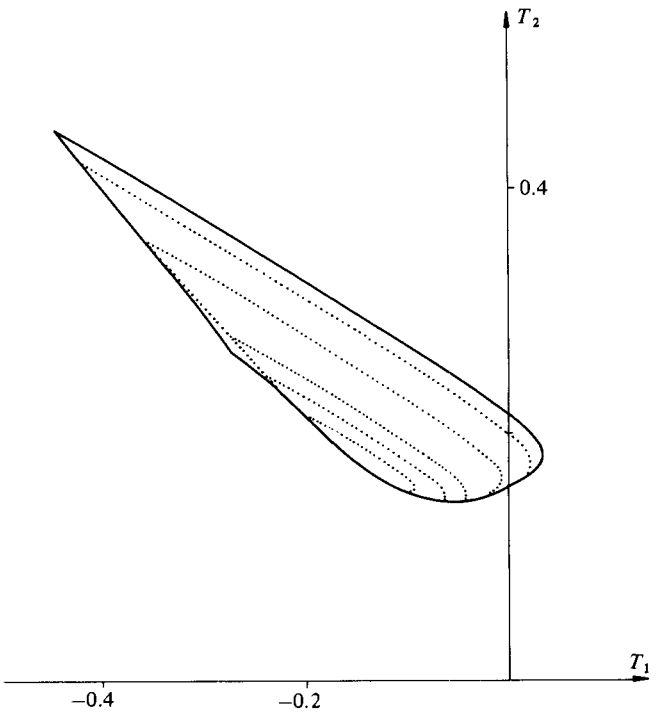

FIGURE 13. Composite phase portrait demonstrating the growth in size of the repelling closed orbits (dotted lines) associated with the supercritically unstable inverse Hopf bifurcation for increasing values of the Rayleigh number $Ra = 100.0, 107.0, 107.73, 107.86$ and 107.8625. The solid line shows the envelope of the associated stable limit cycles.

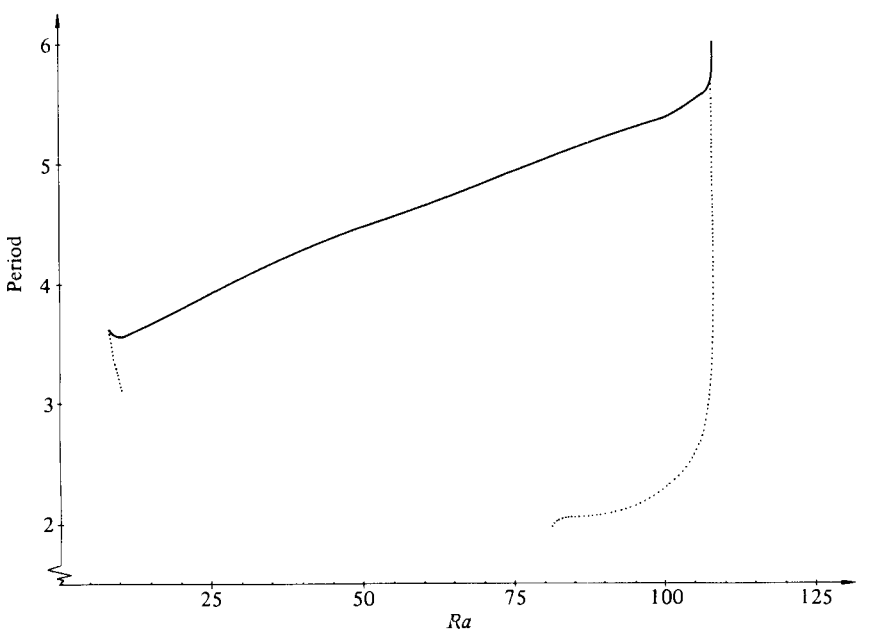

FIGURE 14. Periods of the stable limit cycle (solid line) versus the Rayleigh number. Also included are the periods of the repelling closed orbits associated with the regular and inverse Hopf bifurcations (dotted lines).

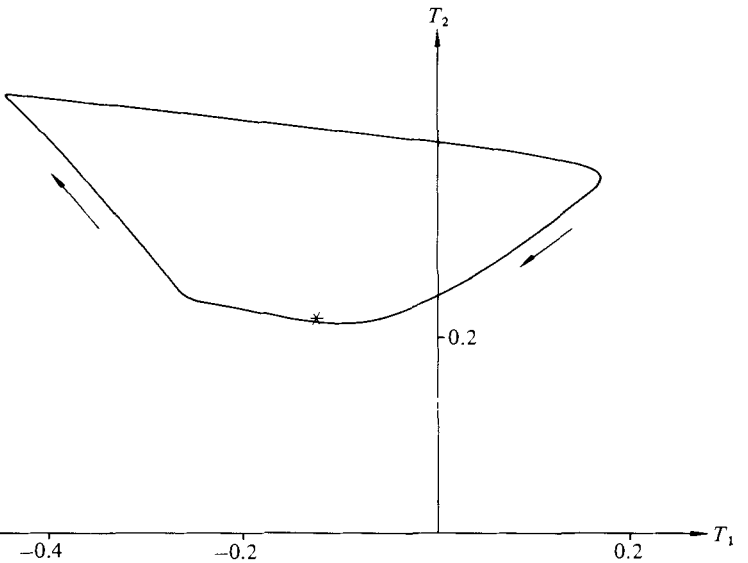

FIGURE 15. Selfsustained oscillation for $Ra = 30$, $Pe = 1$, $\theta = -\frac{5}{6}$ and $\delta = \frac{1}{10}$. The cross shows the position of the critical point.

Analogous computations have been undertaken for the supercritical bifurcation, and the repelling orbits for various values of the Rayleigh number are shown in the composite phase portrait of figure 13 together with the envelope of the corresponding stable limit cycles. The period of the subcritically unstable orbit as it emerged proved to be $T = 3.14$, well in accordance with the theoretical prediction $T = 2\pi/|\lambda(Ra^c)|$, as was the value obtained for the supercritically unstable bifurcation, namely $T = 1.99$. In this context it may furthermore be noted that, even though the resulting unstable orbits modify the relaxation oscillation somewhat, it is not the Hopf bifurcation which gives rise to the nonlinear oscillatory behaviour of the system. (This in marked contrast with such well-known nonlinear oscillations as those associated with van der Pol's triode circuit and Watt's centrifugal governor, both of which are constituted by supercritically stable periodic orbits emerging from regular Hopf bifurcations.)

In figure 14 the non-dimensional period of the relaxation oscillation has been graphed for the entire range of Rayleigh numbers over which self-sustained oscillations take place. Due to the dependence of the position of the attracting paths upon the degree of thermal forcing, the amplitude of the relaxation oscillation increases for large values of the Rayleigh number. Consequently the period of the cycle should also increase, since the motion along the attracting paths is essentially controlled by thermal diffusion, and this is precisely what is observed. The figure also includes the periods of the repelling closed orbits where these occur. An interesting feature of this graph is the tendency towards singular behaviour that is demonstrated by the periods before coinciding at the turning points. This effect is due to the lack of inertia in the system, which in the immediate vicinity of the turning points manifests itself in a tendency of the solutions on the symmetrical attracting path to equilibrate before the onset of instability.

To conclude this subsection it might be noted that the numerical investigations reported above have restricted themselves to the case of $\delta = \frac{1}{2}$. This, however, does

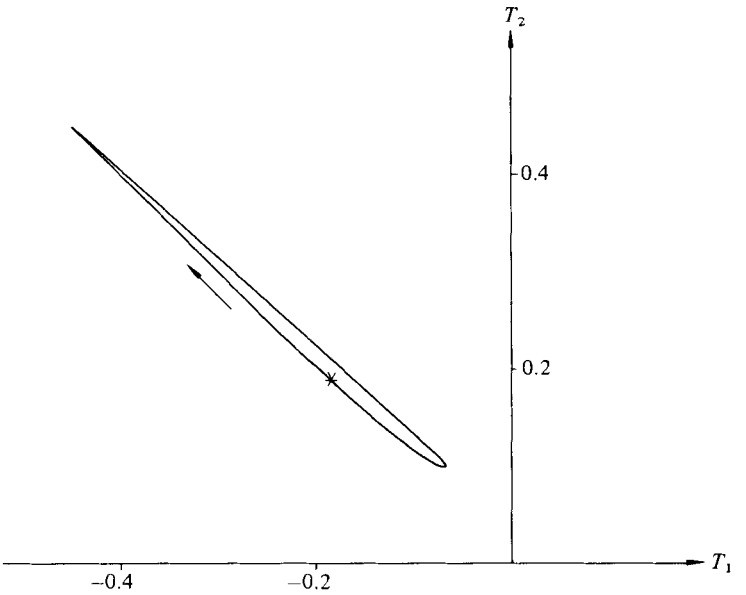

FIGURE 16. As figure 15, but for $Ra = 500$, $Pe = 1$, $\theta = -\frac{85}{86}$ and $\delta = \frac{9}{10}$.

not represent any serious limitation, since for a fixed value of γ the changes of the phase portrait which a varying volume ratio δ gives rise to are solely of a quantitative nature, as is evident from figures 15 and 16. Here the phase portraits of the self-sustained oscillation are shown for $Ra = 30$, $Pe = 1$, $\theta = -\frac{5}{6}$ and $\delta = \frac{1}{10}$ and $Ra = 500$, $Pe = 1$, $\theta = -\frac{85}{86}$ and $\delta = \frac{9}{10}$ respectively. (This choice of parameters yields identical values of γ, whereas the almost-equal ϵ-values correspond to strong thermal forcing within the oscillatory regime.) The qualitative characteristics of these phase portraits can be explained in terms of heat conservation of the fluid during the almost adiabatic jump from the antisymmetrical attracting path, why the shape of the resulting limit cycles to a large extent is determined by the volume ratio of the vessels.

5. Summary and discussion

We have examined the behaviour of stationary and evolutionary solutions to a second-order system of nonlinear autonomous ordinary differential equations representing convective motion of a fluid with a quadratic equation of state. It has been shown that, despite its apparent simplicity, the system can exhibit rather complex modes of behaviour. For both weak and strong thermal forcing it has one stable critical point. The transient adjustment to this stationary solution can, however, be rather circuitous due to the presence of two attracting paths. When the forcing is of intermediate strength the critical point loses its stability and the final state takes the form of a relaxation oscillation. For certain ranges of thermal forcing the solution was found to be nonunique owing to sub- and supercritically unstable periodic orbits emerging from Hopf bifurcations, and thus the final state of the system was dependent upon the initial values. This richness in structure of the possible solutions is perhaps surprising when one considers the very modest nonlinearity in the equation

of state that gives rise to it, but, lest any doubts should linger about the qualitative influence of a quadratic density law, they should be dispelled by considering the results of applying a linear equation of state to the problem. All solutions would in this case adjust themselves to a steady state and no self-sustained oscillation could occur.

Even though the governing equations locally for the abovementioned Hopf bifurcations are analytical, this does not hold true globally for the relaxation oscillation, where instead the non-analytical character of (3.3*a*, *b*) plays a decisive rôle in maintaining the limit cycle. Consequently it appears very unlikely that the present results could be generalized to a continuous system, since the nonanalytical advection terms in the governing equations are due to the imposed spatial homogeneity of the fluid within each of the vessels. Nevertheless, the model investigated here is of interest in its own right and can furthermore serve as a substructure for potentially interesting extensions of the system. Thus a Newtonian heat flux between the vessels can be specified without violating the basic tenet that no spatial dependence within the system be permitted. Further investigations which are being pursued concern the effects of a slackening of the restriction that the conductive properties of the vessels be the same, a restraint originally introduced so as to make feasible an analytical treatment of the problem. Another extension which is being considered is that of including the effects of inertia on the flow. This, however, complicates the situation by yielding a third-order problem, since in this case the equation governing the flow between the vessels will include an acceleration term.

A tacit assumption of all considerations underlying the present theoretical investigation is that the system be experimentally realizable and indeed laboratory work is in progress with the aim of substantiating the qualitative predictions of this paper.

The authors wish to thank Drs L. Arkeryd and R. Krishnamurti for valuable discussions and furthermore acknowledge the constructive comments made by a referee. We are also grateful to the institute staff for efficient help with the technical preparation of the manuscript. The work herein reported was done while one of the authors (P.L.) had a fellowship from the Nordic Universities Group on Physical Oceanography and has been supported by the Swedish Natural Sciences Research Council under contract NFR-G4768-102.

REFERENCES

INCE, E. L. 1926 *Ordinary Differential Equations*. Longmans & Green.

IOOSS, G. & JOSEPH, D. D. 1980 *Elementary Stability and Bifurcation Theory*. Springer.

LANDAU, L. D. & LIFSCHITZ, E. M. 1963 *Fluid Mechanics*. Pergamon.

LASALLE, J. & LEFSCHETZ, S. 1961 *Stability by Liapunov's Direct Method*. Academic.

LEFSCHETZ, S. 1962 *Differential Equations: Geometric Theory*, 2nd edn. Wiley-Interscience.

LORENZ, E. N. 1960 Maximum simplification of the dynamic equations. *Tellus* **12**, 243.

LORENZ, E. N. 1963 Deterministic nonperiodic flow. *J. Atmos. Sci.* **19**, 39.

MARSDEN, J. & MCCRACKEN, M. 1976 *The Hopf Bifurcation and Its Applications*. Springer.

PEDLOSKY, J. & FRENZEN, C. 1980 Chaotic and periodic behaviour of finite-amplitude baroclinic waves. *J. Atmos. Sci.* **37**, 1177.

STOMMEL, H. 1961 Thermohaline convection with two stable regimes of flow. *Deep-Sea Res.* **13**, 224.

STOMMEL, H. & ROOTH, C. 1968 On the interaction of gravity and dynamic forcing in simple circulation models. *Deep-Sea Res.* **15**, 165.

VICKROY, V. G. & DUTTON, J. A. 1979 Bifurcation and catastrophe in a simple forced, dissipative quasi-geostrophic flow. *J. Atmos. Sci.* **36**, 42.

WELANDER, P. 1981 Oscillations in a simple air–water system driven by a stabilizing heat flux. *Dyn. Atmos. Oceans* **5**, 269.